MMP2/9 downregulation is responsible for hepatic function recovery in cirrhotic rats following associating liver partition and portal vein ligation for staged hepatectomy

Yugang Qin[1,2]^, Chonghui Li[3], Xinlan Ge[3], Qiang Zhang[2], Xiaojun Wei[2], Rong Liu[4]

[1]Medical School of Chinese PLA, Beijing, China; [2]Department of Hepatobiliary Surgery, Aerospace Center Hospital, Beijing, China; [3]Institute of Hepatobiliary Surgery, Faculty of Hepato-Pancreato-Biliary Surgery, Key Laboratory of Digital Hepatobiliary Surgery, Chinese PLA General Hospital, Beijing, China; [4]Department of Hepatobiliary, Pancreatic Surgical Oncology, The First Medical Center of Chinese PLA General Hospital, Beijing, China

Contributions: (I) Conception and design: Y Qin, C Li, Q Zhang, X Wei, R Liu; (II) Administrative support: None; (III) Provision of study materials or patients: None; (IV) Collection and assembly of data: Y Qin, X Wei; (V) Data analysis and interpretation: Y Qin, X Ge, Q Zhang, X Wei, R Liu; (VI) Manuscript writing: All authors; (VII) Final approval of manuscript: All authors.

Correspondence to: Rong Liu. Department of Hepatobiliary, Pancreatic Surgical Oncology, The First Medical Center of Chinese PLA General Hospital, 28 Fuxing Road, Beijing 100853, China. Email: liurong301@126.com.

Background: Associating liver partition and portal vein ligation for staged hepatectomy (ALPPS) was introduced in 2007. The current study explored the mechanisms of rapid liver hypertrophy after ALPPS in cirrhotic rats.

Methods: A cirrhotic rat model was constructed and portal vein ligation (PVL) or ALPPS treatments were administered. The liver hyperplasia rate of the rats was calculated, and hepatic function was evaluated using biochemical factors and the indocyanine green excretion test. Subsequently, enzyme-linked immunosorbent assay (ELISA), immunohistochemistry, and hematoxylin and eosin (HE) staining were performed to determine the degree of liver regeneration. Differentially expressed genes during the rapid liver hypertrophy were detected by bioinformatics analysis, followed verification using real-time quantitative polymerase chain reaction (RT-qPCR) and immunohistochemistry.

Results: The body weight of rats that underwent PVL and ALPPS changed during the first 1–4 days postoperatively, and the alterations were more pronounced in rats receiving ALPPS. The recovery of body weight in cirrhotic rats was slower than that in normal rats. The levels of biochemical factors and the indocyanine green retention rate increased 1 day after PVL and ALPPS, and then decreased gradually. PVL and ALPPS elevated the levels of cytokines, inflammatory factors, and proliferating cell nuclear antigen (PCNA) in rats at 1 day postoperatively. HE observation of rat liver condition showed that rats recovered faster within the first 4 days postoperatively. ALPPS surgery resulted in a significant downregulation of matrix metalloproteinase (MMP)2/9 expression in cirrhotic rats at postoperative day 4.

Conclusions: Liver function was partially recovered in cirrhotic rats after ALPPS, and the underlying mechanisms may involve PCNA and MMP2/9.

Keywords: Cirrhosis; associating liver partition and portal vein ligation for staged hepatectomy; matrix metalloproteinases (MMPs); proliferating cell nuclear antigen (PCNA); liver hypertrophy

Submitted Feb 19, 2022. Accepted for publication Apr 11, 2022.
doi: 10.21037/atm-22-1312
View this article at: https://dx.doi.org/10.21037/atm-22-1312

^ ORCID: 0000-0001-8646-2801.

Introduction

Cirrhosis is a late-stage liver disease that is often associated with increased risk of developing primary hepatocellular carcinoma. The triggers and causes of cirrhosis in¬clude viral hepatitis, alcohol consumption, non-alcoholic fatty liver, and toxic substances, which lead to liver fibrosis (1). Treatment options for cirrhosis are limited, and principally concentrate on avoiding complications and progression of disease. However, poor adherence to treatment regimens often results in unfavorable outcomes (2). Hepatectomy is one of the most challenging operations in abdominal surgery due to the multifaceted anatomical arrangement in the liver and the rich blood supply. Furthermore, the challenges associated with cirrhotic liver resection are even greater due to the influence of surgical stress and trauma imposed on borderline liver function and the reduced ability for liver regeneration in cirrhotic livers (3).

Portal vein embolization (PVE) is a conventional regimen to improve the safety of hepatectomy, and contributes to 20–35% hypertrophy in up to 45 days (4,5). However, both PVE and portal vein ligation (PVL) are associated with substantial failure rates, with only approximately two thirds of patients ultimately benefiting from a curative resection (6). More recently, associating liver partition and PVL for staged hepatectomy (ALPPS) has been demonstrated to be a beneficial strategy to stimulate a rapid and obvious augmentation in future liver remnant volume (7). Thus, ALPPS may be a viable option when hypertrophic stimuli attributed to PVL or PVE are not expected to induce sufficient future liver remnant within an acceptable waiting time to advance to the second stage of hepatectomy (8). The principle of ALPPS involves deportalization of liver segments 4 to 8 by integrating PVL of the right portal branch into the parenchyma transection (9). While ALPPS is increasingly recognized, further meticulous evaluation is warranted before its broader clinical application. In particular, the underlying mechanisms of ALPPS-induced liver regeneration should be elucidated (10). While ALPPS is a well-recognized surgical modality for unresectable colorectal liver metastasis (11), its role in cirrhosis has been less studied. A previous report demonstrated that genes in the interleukin-6 (IL-6)-tumor necrosis factor-α (TNF-α)-STAT3 signaling pathway were expressed at significantly higher levels after ALPPS step I compared to PVL alone (12), suggesting a possible association between pro-inflammatory cytokines and ALPPS. This current study explored the molecular changes during ALPPS and the effects of ALPPS and PVL in a cirrhosis model using rats. We present the following article in accordance with the ARRIVE reporting checklist (available at https://atm.amegroups.com/article/view/10.21037/atm-22-1312/rc).

Methods

Animals

A total of 171 8-week-old male Sprague-Dawley rats (280–300 g, Beijing Vital River Laboratory Animal Technology Co., Ltd., Beijing, China) were maintained for 1 week in chip-bedded cages at a temperature of 24±1 ℃, in a light-controlled room (12-h light/dark cycles). Animals were allowed free access to water and standard rat chow, 4 rats per cage and received humane care. After 1 week, the rats were weighed to ensure that the weight differences between animals were within 10 g. A protocol was prepared before the study without registration. Experiments were performed under a project license (No. 20200511-JJJHZ-01) granted by the Medical Ethics Committee of Aerospace Center Hospital, in compliance with Chinese guidelines for the care and use of animals.

Establishment of the cirrhotic rat model

Rats were injected subcutaneously with carbon tetrachloride (CCL4) solution (mixed with olive oil at 1:1 by volume) at 0.5 mL/100 g twice a week for 12 weeks. The condition of the rats was closely observed. Successfully generated cirrhotic rats (C group) were maintained and fed for the following assays.

Enzyme-linked immunosorbent assay (ELISA)

The serum levels of recombinant human hepatocyte growth factor (HGF), transforming growth factor-β (TGF-β), tumor necrosis factor (TNF)-α, and interleukin (IL)-6 in rats were detected by ELISA kits (Elabscience Biotechnology Company, Co., Ltd., China). Whole blood samples were collected in tubes and allowed to stand for 2 hours at 4 ℃. Samples were centrifuged at 1,760 g for 10 minutes to obtain the supernatant. The serum was frozen at –80 ℃ and elective unified testing after all surgical procedures have been completed. Samples (100 μL) were transferred to a 48-well plate and incubated with detection reagent for 90 minutes, followed by 90 μL tetramethylbenzidine for 15 minutes in the dark (both at

37 ℃). The reaction was terminated with the addition of 50 μL termination solution and the optical density (OD) was measured at 450 nm using a microplate reader (DECAN, Decna Trading Co., Ltd., Shanghai, China).

Real-time quantitative polymerase chain reaction (RT-qPCR)

Total RNA was isolated from liver tissues using RNAsimple Total RNA Kits (Tiangen, Biotech, Beijing, China). Total RNA (1 μg) was reverse transcribed into complementary deoxyribonucleic acid (cDNA) using RevertAid first strand cDNA synthesis kit (Thermo Fisher Scientific, USA). To quantify mRNA expression of matrix metalloproteinase (MMP)2 and MMP9, RT-qPCR was performed with an SYBR Premix Ex Taq II (TaKaRa Bio Inc., Dalian, China) using a StepOnePlus Real-Time PCR system (Applied Biosystem, CA, USA). The results of the RT-PCR were normalized to glyceraldehyde-3-phosphate dehydrogenase (GAPDH). The RT-PCR primer sequences used are as follows: MMP2 forward: 5'-GTGAAGTATGGGAACGCCG-3', reverse: 5'-GCCGTACTTGCCATCCTTCT-3'; MMP9 forward: 5'-GGCGTGTCTGGAGATTCG-3', reverse: 5'-TACTGGAAGATGTCGTGTGAG-3'; GAPDH forward: 5'-CCACAGTCCATGCCATCAC-3', reverse 5'-CGTTCAGCTCAGGGATGAC-3'.

Detection of liver function indexes

After the operation, rats were anesthetized with 1% pentobarbital sodium at 90 mg/kg via intraperitoneal injection at the indicated time point, and the inferior vena cava was exposed after laparotomy. Venous blood (3 mL) was collected from the inferior vena cava of each rat, and the supernatant was harvested after a 10-minute centrifugation at 1,760 g at 4 ℃. The levels of alanine transaminase (ALT), aspartate transaminase (AST), albumin (ALB), total protein (TP), and total bilirubin (TBIL) in rat serum were measured using an automatic biochemical analyzer (Olympus Optical Co., Ltd., Tokyo, Japan).

Hematoxylin-eosin (HE) staining

Animal were placed under 1% pentobarbital sodium maintenance anesthesia and the liver was collected. Liver specimens were fixed in 4% paraformaldehyde at room temperature for 24 hours, paraffin-embedded and cut into 4-μm thick sections. The sections were dewaxed, hydrated, and stained with hematoxylin and eosin for 5 minutes and 1 minute, respectively, using the ST Infinity H&E Staining System (Leica Biosystems, USA) at room temperature for histopathological examination. The sections were then embedded, and five random fields of view were observed and photographed using a BX63F optical microscope (Olympus Corporation).

Modeling and grouping of rats

A total of 81 untreated rats (N group) and 90 cirrhotic rats (C group) were randomly divided into the following 4 groups: no treatment group (n=6), sham-operated group (S group, n=25), PVL group (P group, n=25), and ALPPS group (A group, n=25). Rats in the S group were administered 1% pentobarbital sodium (90 mg/kg) for laparotomy and perihepatic mobilization. After anesthesia, rats in the P group were fixed in a supine position on a self-made operating table. A 5-cm long transverse incision was created at the median part of the upper abdomen, and the perihepatic ligament was mobilized to fully expose the liver. The portal vein branches of the right lobe branch, left side of the middle lobe, left lobe branch, and caudate lobe branch were ligated with 7-0 silk sutures. After the ligation was completed, the abdominal cavity was rinsed with normal saline and closed layer by layer. For rats in the A group, portal vein branches were first ligated after anesthesia as described above (defined as ALPPS I). Thereafter, the dorsal membrane of the liver along the right side of the sickle ligament was dissected using scissors, and the liver parenchyma was separated layer by layer along the left side of the ischemic line with a coagulant pen until the inferior vena cava (defined as ALPPS II). The abdominal cavity was then rinsed with saline and closed layer by layer (13).

All rats fasted for 12 hours before surgery, with free access to drinking water. The time of operation and time of recovery of the rats were recorded. Bleeding in the rats was controlled by electrocoagulation or compression hemostasis and wiped with gauze or cotton swabs. The weight of the wet gauze was weighed and the weight of dry gauze was subtracted to calculate the blood loss. The rats were kept in cages after the operation and 5 rats were taken out on the 1st, 4th, 7th, 10th, and 14th day. The indocyanine green (ICG) excretion rate was measured at 5 observation points on the 1st, 4th, 7th, 10th, and 14th day after ALPPS, followed by intraperitoneal injection of 1% sodium pentobarbital (150 mg/kg) to euthanize the rats. After the experiment, the

rats were sacrificed by exsanguination.

At the end of the experiment, the rat liver was harvest and weighed. The future liver remnant (FLR) was weighed immediately after removal of the attached ligaments, portal veins, and other tissues. The liver hyperplasia rate = (postoperative FLR weight – predicted preoperative FLR weight)/predicted preoperative FLR weigh × 100%.

The indocyanine green (ICG) excretion rate

The ICG was completely dissolved in distilled water and prepared to a final concentration of 5 mg/mL. Each rat was injected with ICG at 0.5 mg/kg in the penile vein. After 15 minutes, blood was collected from the inferior vena cava by puncture, transferred into a heparinized tube, and centrifuged at 1,500 g for 15 minutes. The plasma (0.25 mL) was diluted with 1.25 mL saline. The optical density (OD) values of the plasma samples at 805 nm were determined by UV-2100 spectrophotometer (UNIC, Unic Instrument Co., Ltd., Shanghai, China) and compared with those of normal plasma. A standard curve was used to calculate the serum concentration of ICG.

Immunohistochemistry

The Polink-2 Plus-horseradish peroxidase (HRP) IgG detection system (ZSGB-Bio, Beijing, China) was utilized for immunohistochemistry, and liver sections were treated with paraffin and rehydrated in ethanol. After 2.5 minutes of repair with citrate buffer at 120 ℃, the sections were incubated with 3% hydrogen peroxide for 10 minutes at room temperature. Sections were incubated overnight with rat antibodies against proliferation cell nuclear antigen (PCNA, ZM-0213, ZSGB-Bio, Beijing, China) and MMP2 (ab86607, 1:500, Abcam), and rabbit antibodies against MMP9 (ZA-0562, ZSGB-Bio, Beijing, China) at 4 ℃. The sections were incubated with HRP-coupled IgG (Kit-5030, Maixin Biotech. Co., Ltd., Fujian, China) for 15 minutes at room temperature. The sections were then stained with diaminobenzidine solution and counter-stained with hematoxylin. Following dehydration and embedding, the sections were observed under a BX63F optical microscope (Olympus).

Bioinformatics analysis

The GSE63742 dataset (regenerating liver at 9 time points at 2, 6, 12, 24, 30, 36, 72, 120, and 168 hours after partial hepatectomy) was downloaded from the Gene Expression Omnibus (GEO) database (https://www.ncbi.nlm.nih.gov/geo). The gene expression profile of rat liver tissues was also measured using a rat Genome 230 2.0 gene microarray, and the experiment was repeated three times at each time point (with data at 0 hours as the control group). All data were normalized using Affymetrix GCOS 2.0 software (Affymetrix, Santa Clara, CA, USA), and volcano plots were plotted using $|P<0.01|$, Log_2Foldchange >1.5. Gene ontology (GO) enrichment of genes was performed by ClusterProfiler package (R, USA), and GO biological pathway annotation information was downloaded from the GO database (http://www.bioconductor.org/packages/release/data/annotation/). Protein-protein interactions (PPI) network construction was performed using the STRING website (https://string-db.org).

Statistical analyses

Statistical analysis was performed using SPSS 25.0 software (IBM SPSS Statistics, Chicago, IL, USA). A P value <0.05 was considered statistically significant. All quantitative variables were presented as the mean ± standard deviation (SD) and compared using unpaired *t*-test or two-way analysis of variance (ANOVA).

Results

A rat model with cirrhosis is successfully established

A total of 90 rats were subjected to subcutaneous injections of 50% CCL_4 and monitored for 12 weeks. At week 4, 1 rat developed ascites, and at week 9, 2 rats showed severe adhesion. By week 12, 3 rats died due to liver failure. These rats were euthanized and excluded from the study. No significant intraperitoneal injury was observed in these rats and therefore, their abnormalities were considered to be due to individual dose intolerance caused by intraperitoneal injections of CCL_4. At the end of 12 weeks, all remaining rats showed cirrhotic nodules and were diagnosed with cirrhosis (stage IV). The modeling success rate was 93.33%. Out of the 84 cirrhotic rats, 81 rats were randomly chosen for subsequent experiments. For cirrhotic and normal rats (n=81), 6 rats were used to compare biochemical indexes, such as AST, ALT, ALB, TBIL and DBIL. There was an increase in AST and ALT levels in cirrhotic rats compared to normal rats, however, the increase in AST levels was not significantly different between the 2 groups (*Figure*

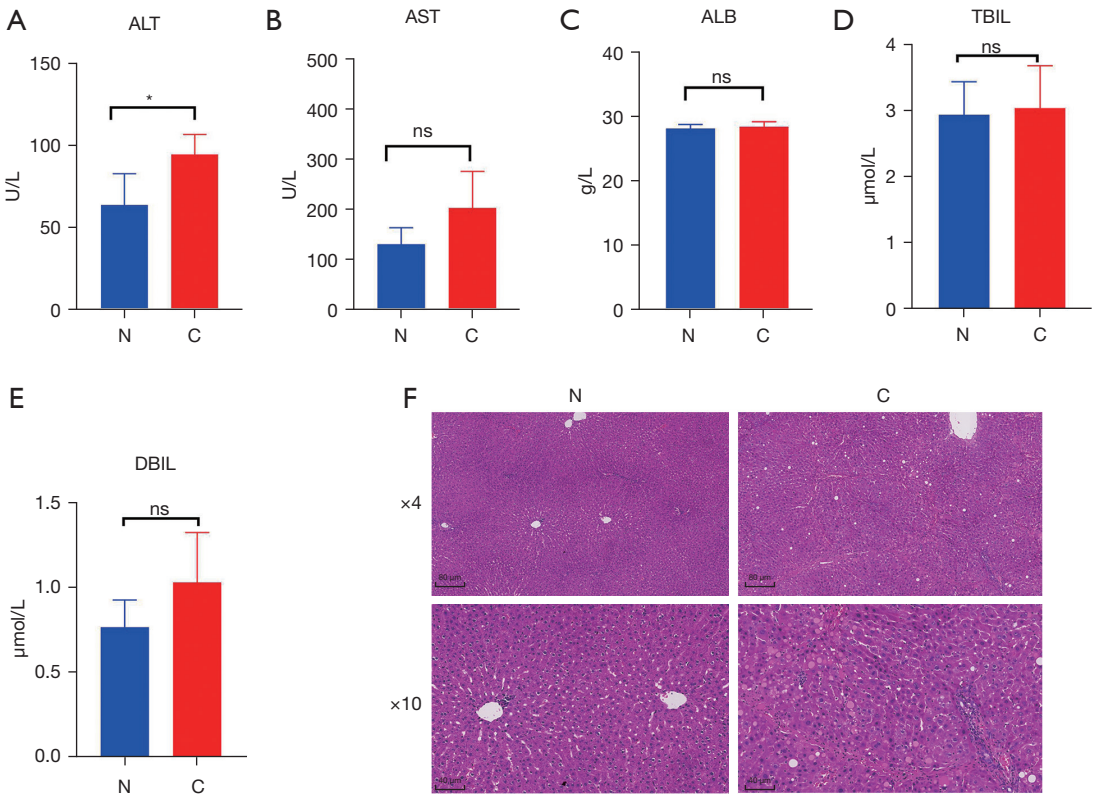

Figure 1 The rat model of cirrhosis was successfully induced. (A-C) Biochemical analysis showing the changes in the levels of serum ALT (A), AST (B), ALB (C), TBIL (D), and DBIL (E) in rats. (F) Hematoxylin and eosin staining of the rat liver tissues (×4 and ×10 magnification, ×4: 1 cm: 80 μm; ×10: 1 cm: 40 μm). All quantitative variables are presented as mean ± standard deviation and data were compared using the Student's *t* test. *, P<0.05; ns, P>0.05. N, untreated; C, cirrhotic; AST, aspartate transaminase; ALT, alanine aminotransferase; ALB, albumin; TBIL, total bilirubin; DBIL, direct bilirubin.

1A,*1B*). There was no significant difference in the levels of ALB, TBIL, nor direct bilirubin (DBIL) between the 2 groups (*Figure 1C-1E*). Liver sections of the control rats demonstrated normal lobular structure, while liver sections of the cirrhotic rats showed typical structural aberrations, and the regenerated nodules were surrounded by proliferative connective tissue, showing typical symptoms of cirrhosis (*Figure 1F*). These results demonstrated the successful construction of the cirrhotic rat model.

Pathological changes after ALPPS and PVL

The remaining 75 cirrhotic rats were subjected to sham operation (CS group, n=25), PVL (CS group, n=25), or ALPPS (CA group, n=25). As a control, 75 normal rats underwent the same procedures of sham operation (NS group, n=25), PVL, (NP group, n=25), or ALPPS (NA group, n=25). All operations were successful. The operation time was recorded, and the blood loss of rats was measured. Rats were maintained in different cages according to the different groups and the time to recovery was recorded. During PVL surgery, there is little bleeding. However, PVL is more difficult in cirrhotic rats. Bleeding during ALPPS mainly occurred when the liver parenchyma was severed, and a hemostatic device with strong electrocoagulation was used to control the bleeding. On 7th, 10th, and 14th day, the operation was more difficult due to adhesion, and the time to separate the adhesion was also longer. During the observation period, it was noted that the cirrhotic rats acquired a longer operation time and recovery time was also prolonged (*Table 1*).

After successful operation, the rats were euthanized at 5 observation points on the 1st, 4th, 7th, 10th, and 14th days, to determine the average body weights (n=5 for each time point). The rat liver tissues were removed, weighed, and analyzed for morphological changes to the liver. Rats in the

Table 1 Details of the rats during the operations

	NS group	NP group	NA group	CS group	CP group	CA group
Duration of surgery (min)						
PVL		19.8±3.46			18.8±2.35	
ALPPS			29.4±4.3*			30.7±5.06*
Recovery time (h)	5.01±1.13	5.25±2.77	5.61±2.94	5.58 ± 2.56	8.03±2.18#	8.52±3.64#

*, P<0.05 comparing A group and P group; #, P<0.05, CA group *vs.* NA group, or CP group *vs.* NP group. Data are present as mean ± SD. PVL, portal vein ligation; ALPPS, associating liver partition and portal vein ligation for staged hepatectomy; NS, normal rats sham operation; NP, normal rats PVL; NA, normal rats ALPPS; CS, cirrhotic rats sham operation; CP, cirrhotic rats PLV; CA, cirrhotic rats ALPPS; SD, standard deviation..

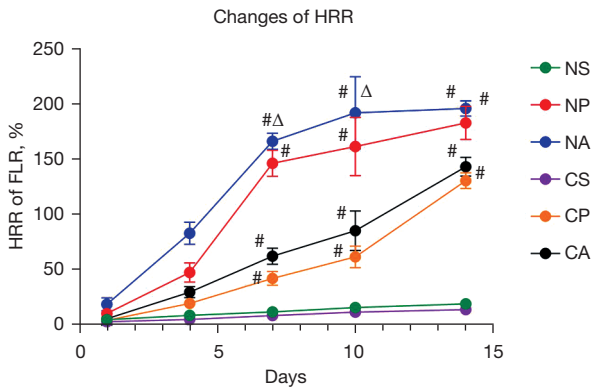

Figure 2 The effects of hepatic regeneration rate following PVL and ALPPS on rats. All quantitative variables are presented as mean ± standard deviation and compared using two-way ANOVA. #, A or P groups *vs.* S groups, P<0.05; Δ, CA group *vs.* NA group. HRR, hepatic regeneration rate; PVL, portal vein ligation; ALPPS, associating liver partition and portal vein ligation for staged hepatectomy; ANOVA, analysis of variance; A, ALPPS; P, PVL; S, sham operated; CA, cirrhotic rats that underwent ALPPS; NA, normal rats that underwent ALPPS.

S groups experienced less weight loss postoperatively, and recover faster than rats in the C or A groups. Rats in the P and A groups showed initial weight loss, followed by weight gain on day 7. The body weight of rats in the A groups decreased gradually between 1–4 days. By day 7, the weight of rats in the A groups was higher than that observed at day 4, and at day 14, the weight was higher than that of rats in the P groups, and higher than the average preoperative weight. The weight of rats in the C groups was lower than that in the N groups, which indicated that the weight recovery ability of cirrhotic rats was weaker than that of normal controls, and the weight recovery ability of rats after ALPSS operation was weaker than that after PVL operation. The rat livers were obtained by dissection, and the liver hyperplasia rate was calculated by measuring the remaining weight of the liver. The liver hyperplasia rate of all three groups of rats was found to increase at different time points. The liver hyperplasia rate of rats in the A groups was faster during days 1–7, while after 7 days, due to insufficient blood supply, the rise of the liver hyperplasia rate slowed down. Rats in the P groups showed a downward trend in the liver hyperplasia rate on day 4, while the rats in the S groups showed a lack of any significant change in the liver hyperplasia rate. The residual liver weight in rats in the C groups was much lower than that of rats in the N groups, indicating that liver cirrhosis, to some extent, hindered the compensatory hyperplasia of the liver (*Figure 2*).

The postoperative liver function in rats

The changes in liver function in rats after PVL and ALPPS were examined. The AST and ALT levels increased significantly after PVL and ALPPS, but decreased significantly on the 4th postoperative day, and continued to decrease with time. The levels of AST and ALT decreased most significantly in cirrhotic rats after PVL, while the AST and ALT levels remained high in cirrhotic rats after ALPPS (*Figure 3A,3B*). Cirrhotic rats exhibited elevated serum ALB levels (not significantly) 7 days after the sham operation. The ALPPS operation reduced ALB levels, while PVL operation did not change ALB levels (*Figure 3C*). TP levels decreased on the 7th day after ALPPS in cirrhotic rats, then increased gradually. By contrast, TBIL levels were elevated after ALPPS in cirrhotic rats, and gradually decreased (*Figure 3D,3E*). The retention rate of ICG diminished significantly and the excretion capacity of ICG increased after PVL and ALPPS. The retention rate of ICG in cirrhotic rats was always higher than that of normal rats,

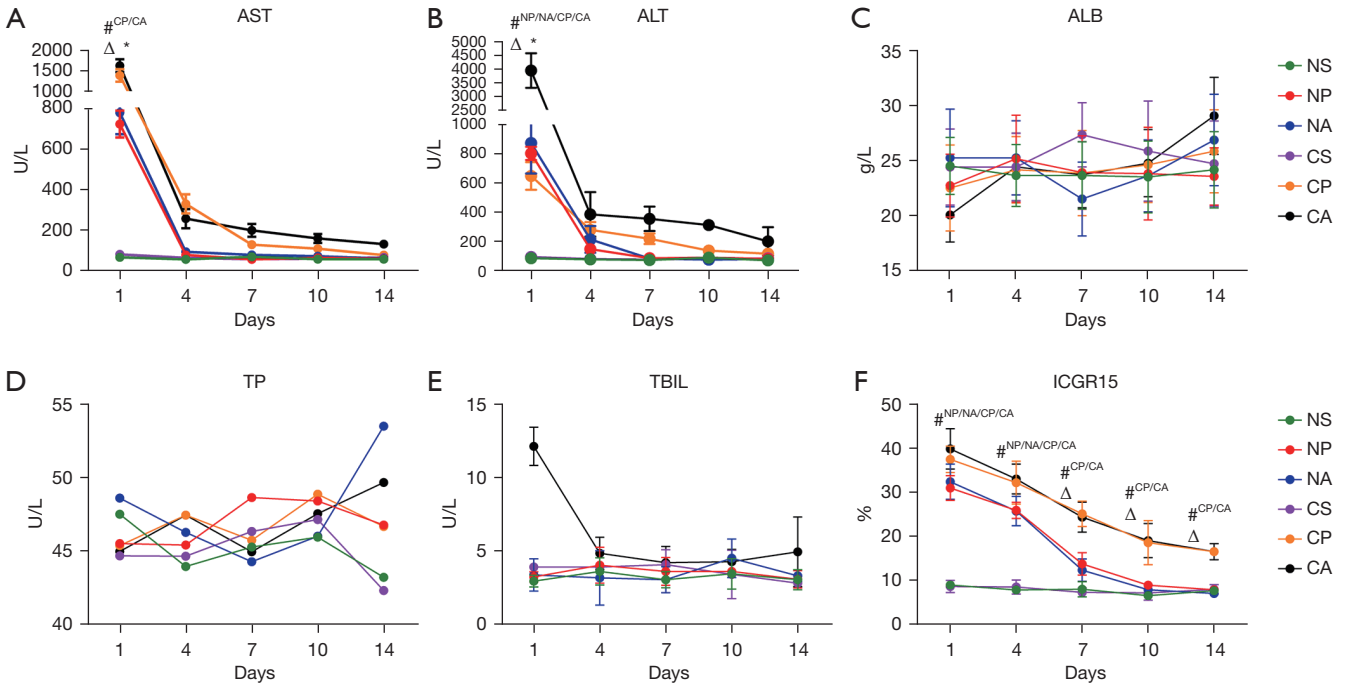

Figure 3 Detection of liver function in rats. Biochemical analysis showing the changes in serum AST (A), ALT (B), ALB (C), TP (D), and TBIL (E) in rats. (F) Detection of hepatic storage capacity of rats by ICG assay. All quantitative variables are presented as mean ± standard deviation and compared using two-way ANOVA. #, A or P groups *vs.* S groups, P<0.05, marked as #NA, #NP, #CP, #CA; Δ, CA group *vs.* NA group, P<0.05; *, CP groups *vs.* CA groups. AST, aspartate transaminase; ALT, alanine aminotransferase; ALB, albumin; TP, total protein; TBIL, total bilirubin; ICG, indocyanine green; ANOVA, analysis of variance; PVL, portal vein ligation; ALPPS, associating liver partition and portal vein ligation for staged hepatectomy; A, ALPPS; P, PVL; S, sham operated; CA, cirrhotic rats that underwent ALPPS; NA, normal rats that underwent ALPPS; CP, cirrhotic rats that underwent PVL.

and the liver function was poorer than that of normal rats (*Figure 3F*). The above liver function tests suggested that ALPPS operation resulted in a significant recovery of liver function in rats at 4–7 days postoperatively, and thereafter, the rate of liver function recovery slowed down. However, liver cirrhosis may weaken the liver function recovery ability of rats after ALPPS operation. Receiving PVL surgery was also conducive to liver function in rats, but it is not as effective as ALPPS surgery.

Postoperative liver hypertrophy in rats

The liver hypertrophy of rats was assessed by measuring the levels of cytokines and inflammatory factors. At postoperative day 4, the levels of HGF increased markedly, then decreased gradually. Furthermore, the HGF levels in cirrhotic rats was higher than that in normal rats (*Figure 4A*,*4B*). The inflammatory factors IL-6 and TNF-α increased first and then decreased in rats after the operation. The levels of inflammatory factor in rats in the P groups were lower than those in the A groups. Cirrhosis had little effect on inflammatory factors in rats (*Figure 4C*,*4D*). The PCNA levels in the rat liver were detected by immunohistochemistry to evaluate the cell division cycle. The expression of PCNA increased significantly from 1 to 4 days postoperatively, then decreased gradually. The PCNA expression in rats in the A groups was higher than that in rats in the P groups. At the same time, cirrhosis at least partially inhibited PCNA expression (*Figure 4E*). HE staining was performed to examine the livers of rats at different time points. On the first postoperative day, the hepatocytes of cirrhotic rats showed severe swelling, widening of hepatic sinus, and congestion. Normal rats showed a smaller degree of pathological change, but a slight degeneration of hepatocyte granules was observed. The necrosis of cells in PVL rats was milder than in ALPPS rats, and inflammatory cell infiltration appeared in the liver 4 days after the operation. Fat deposition and interstitial hyperplasia were observed in cirrhotic rat livers.

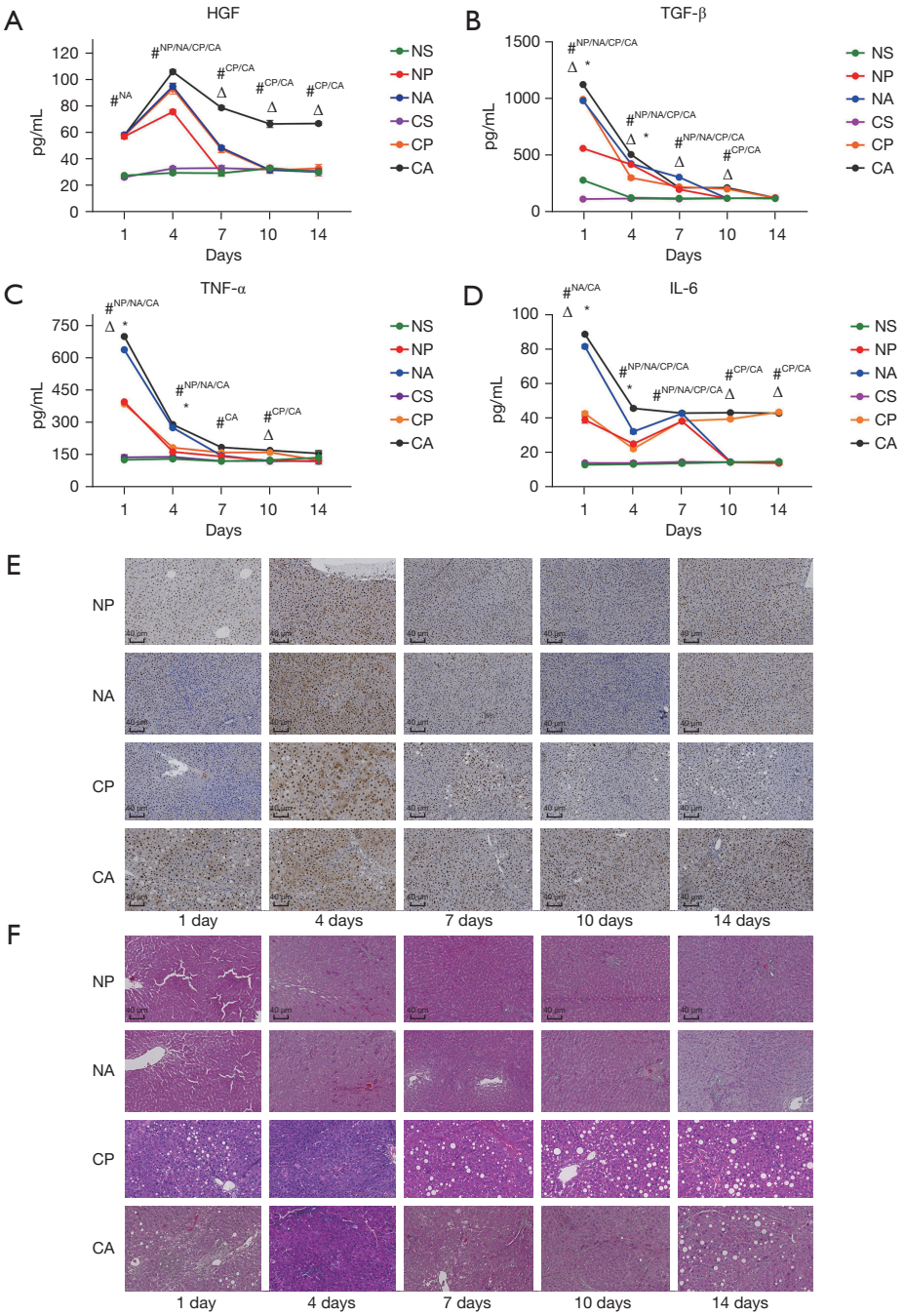

Figure 4 Detection of liver hypertrophy in rats after the operation. ELISA assay showing the changes in expression of HGF (A), TGF-β (B), TNF-α (C), and IL-6 (D) in rats. (E) The PCNA levels in rat livers were assessed by immunohistochemistry (×10 magnification, ×10: 1 cm: 40 μm). (F) Hematoxylin and eosin staining of rat liver tissues (×10 magnification, ×10: 1 cm: 40 μm). All quantitative variables are presented as mean ± standard deviation and compared using two-way ANOVA. P<0.05. $^{\#}$, A or P groups *vs.* S groups, P<0.05, marked as #NA, #NP, #CP, #CA; $^{\Delta}$, CA group *vs.* NA group, P<0.05; *, CP groups *vs.* CA groups. ELISA, enzyme-linked immunosorbent assay; HGF, hepatocyte growth factor; TGF, transforming growth factor; TNF, tumor necrosis factor; IL, interleukin; PCNA, proliferating cell nuclear antigen; ANOVA, analysis of variance; PVL, portal vein ligation; ALPPS, associating liver partition and portal vein ligation for staged hepatectomy; A, ALPPS; P, PVL; S, sham operated; CA, cirrhotic rats that underwent ALPPS; NA, normal rats that underwent ALPPS; CP, cirrhotic rats that underwent PVL.

For rats in the CA group, the hepatic sinuses narrowed and congestion decreased. After 7–14 days, it was observed that the liver of CA rats gradually returned to a normal state, and NA rats showed the best recovery. CP rats had poor recovery, with hepatocyte balloon-like changes in the liver (*Figure 4F*). A degree of hypertrophy was observed in rat livers after ALPPS and PVL. Nonetheless, liver recovery was superior after ALPPS operations, and cirrhotic rats had a certain degree of hypertrophy and recovery after ALPPS operations.

Differentially expressed genes before and after ALPPS in rats

Since liver function and proliferation-related genes in rats changed significantly at postoperative day 4, the differentially expressed genes before and after PVL and ALPPS were examined. Analysis of the GSE63742 dataset revealed that the gene expression at 36 hours after hepatectomy differed most significantly from that at 0 hours (*Figure 5A*). Analysis of the differentially expressed genes after 36 hours of liver regeneration showed that 355 genes were significantly upregulated and 529 genes were significantly downregulated (*Figure 5B*). To determine the functional gene clusters that play a role in liver regeneration, GO enrichment (biological processes) analysis was conducted, with 42 genes directly involved in the regulation of regeneration (*Figure 5C*). Exploring the interrelationship of these genes through the PPI network revealed two major gene clusters in the regeneration process, a proliferative cycle process centered on PCNA and a stromal proliferation process centered on MMPs (*Figure 5D*). *Figure 4E* shows the PCNA expression. The expression of MMP2/MMP9 in liver tissue from each group of rats was analyzed by RT-qPCR. The expression of MMP2 and MMP9 were downregulated on the 1st day and upregulated on the 10th day. The most significant downregulation was observed in the NA group (*Figure 5E*). Immunohistochemistry revealed that MMP2 had the highest protein expression on day 14 in the CA group, but decreased significantly on days 1–4 (*Figure 5F*). The change in IOD value in MMP9 was not as obvious as that in MMP2, but it can be seen that the protein expression decreased first and then increased (*Figure 5G*). Therefore, MMP2 and MMP9 are key genes for liver function and hypertrophy in rats after ALPPS.

Discussion

This study evaluated hypertrophy in cirrhotic and normal rats undergoing the novel ALPPS two-stage hepatectomy and PVL alone, and examined the possible underlying mechanisms. Our study proposed that a considerable amount of hypertrophy was achieved even in rats with cirrhosis after ALPPS. After successful construction of the cirrhotic rat model, normal and cirrhotic rats were subjected to sham operation, PVL, or ALPPS. Although recovery of body weight was weaker in rats that underwent ALPPS compared to rats receiving PVL, the liver hyperplasia rate was much higher. At the same time, cirrhotic rats that underwent ALPPS exhibited lower liver hyperplasia rates than normal rats that underwent ALPPS. Linecker *et al.* observed that partial ALPPS with a median partial transection of 61% led to equivalent future liver remnant hypertrophy relative to a complete parenchymal transection (14). Recent data provided by Chan *et al.* indicated that the extent of liver hypertrophy in ALPPS I (PVL, 69%) is superior to PVE alone (50%) (15). Moreover, extensive hypertrophy was noted in patients with low-grade fibrosis, and a noticeably smaller degree of hypertrophy was induced in cirrhotic livers, which may decrease liver hypertrophy by up to 50% (16). More specifically, ALPPS surgery in patients with cirrhosis resulted in sustained proliferation and accelerated second stage hepatectomy within a short time. Meanwhile, in the normal liver, days 1 and 3 after ALPPS tend to be the cardinal periods for liver regeneration, with the rate of liver regeneration decreasing after 7 days (17). Indeed, ALPPS augmented liver regeneration to the point where increases in standardized future liver remnant and liver-to-body-weight-ratio were sufficient for a resection after a median of 9 days (18). In the normal liver, ALPPS surgery was associated with more extensive liver growth compared to PVL surgery (19). Liver regeneration after ALPPS in cirrhotic livers lagged behind that of normal livers (20). These aforementioned reports were largely consistent with our findings showing that the liver hyperplasia rate increased significantly during days 1–7 after ALPPS, and thereafter, slowed down. Therefore, while there is a considerable risk in cirrhotic patients, ALPPS remains a salvage option in selected patients with cirrhosis, in whom PVE has been ineffective (21).

One of the potential mechanisms involves parenchymal transection, which disturbs intrahepatic portal collaterals and may induce inflammation, thereby releasing putative growth factors and constituting a regeneration stimulus (22). Our observations revealed that HGF, TGF-β, IL-6, TNF-α, and PCNA all showed an upward trend after ALPPS and gradually reduced. While there is little cell division in

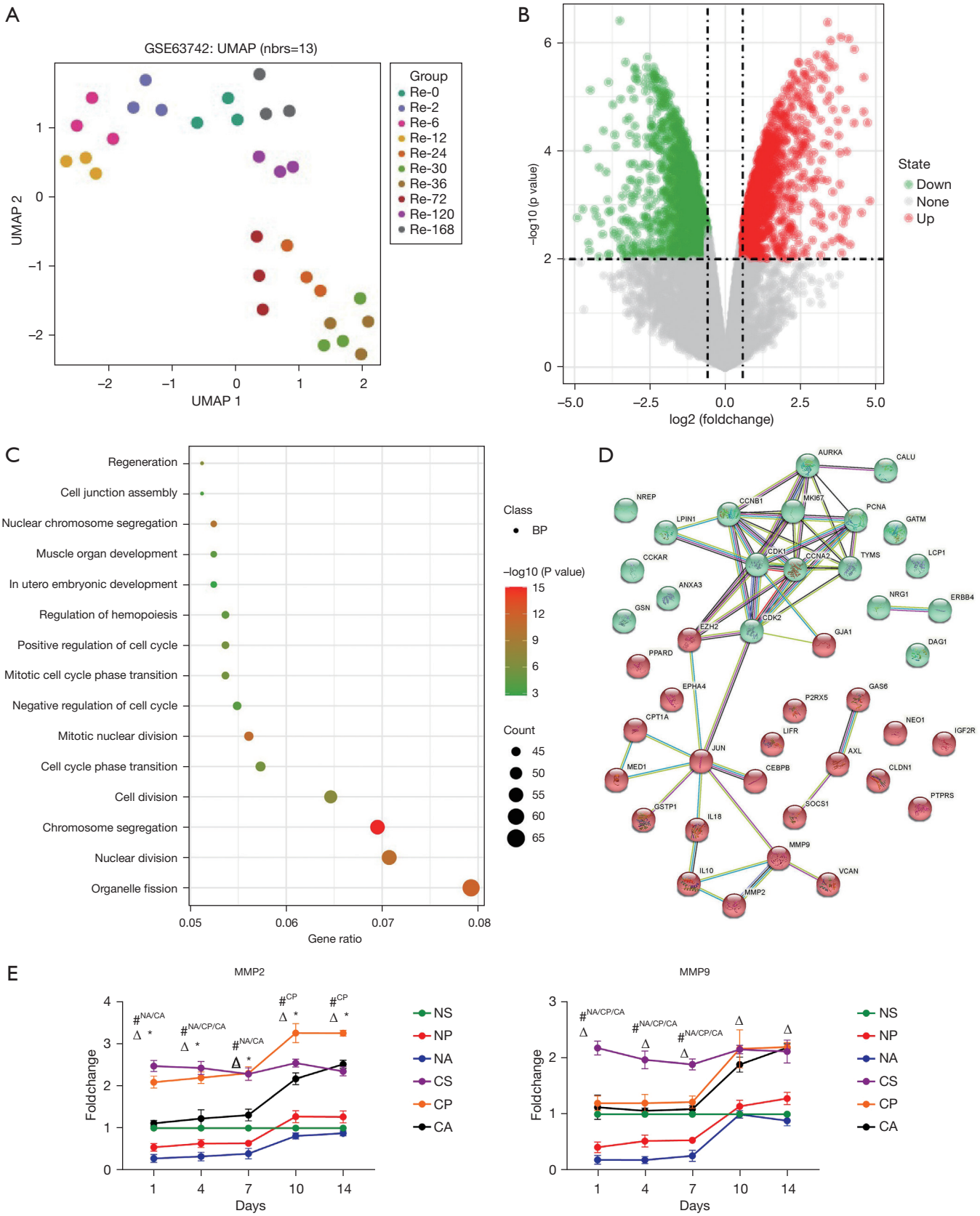

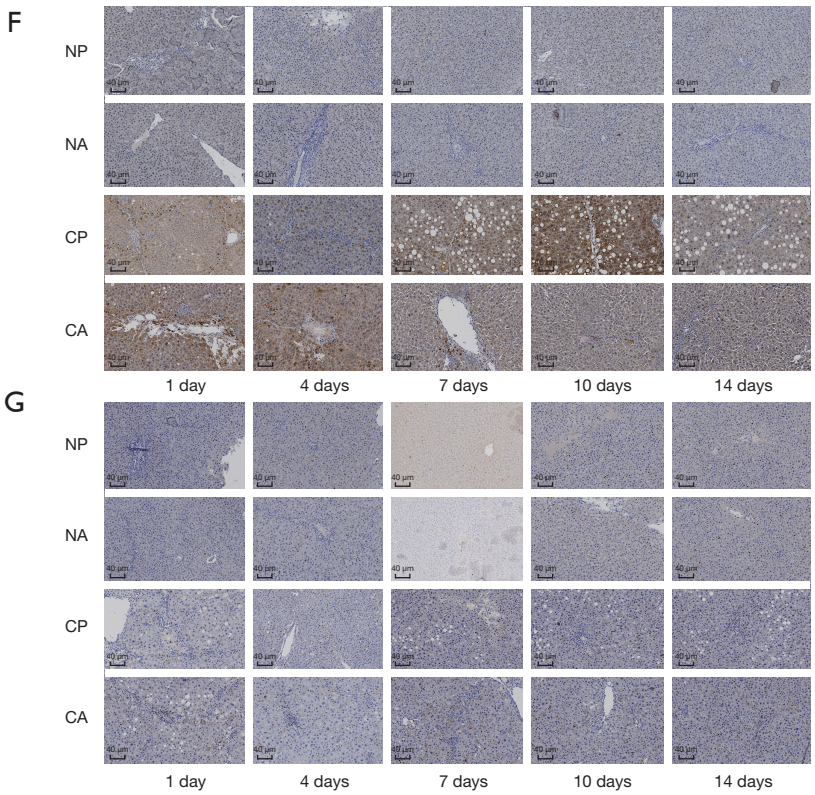

Figure 5 The main genes responsible for liver changes following ALPPS. (A) Three biological replicate differences for each group of experiments visualized using UMAP. (B) A volcano plot showing the changes in gene expression after 36 hours of liver hyperplasia. (C) GO enrichment analysis showing the biological process of the differentially expressed genes in the GSE63742 dataset. (D) The PPI analysis on the differentially expressed genes in the GSE63742 dataset. (E) The expression of MMP2 and MMP9 in rat tissues as determined by RT-qPCR. (F) The expression of MMP2 in tissues was assessed by immunohistochemistry (×10 magnification, ×10: 1 cm: 40 μm.). (G) The expression of MMP9 in tissues was assessed by immunohistochemistry (×10 magnification, ×10: 1 cm: 40 μm.). All quantitative variables are presented as the mean ± standard deviation and compared using two-way ANOVA. P<0.05. $^{\#}$, A or P groups *vs.* S groups, P<0.05, marked as #NA, #NP, #CP, #CA; $^{\Delta}$, CA group *vs.* NA group, P<0.05; *, CP groups *vs.* CA groups. ALPPS, associating liver partition and portal vein ligation for staged hepatectomy; GO, Gene Ontology; MMP, matrix metalloproteinase; RT-qPCR, real-time quantitative polymerase chain reaction; ANOVA, analysis of variance; PVL, portal vein ligation; A, ALPPS; P, PVL; S, sham operated; CA, cirrhotic rats that underwent ALPPS; NA, normal rats that underwent ALPPS; CP, cirrhotic rats that underwent PVL; CA, cirrhotic rats that underwent ALPPS; UMAP, Uniform Manifold Approximation and Projection.

hepatocytes of normal adult livers, after partial hepatectomy, around 95% of hepatic cells rapidly re-enter the cell cycle. In the rat liver, the rate of DNA synthesis in hepatocytes starts to elevate after approximately 12 hours and peaks at about 24 hours (23), which may explain the elevation of PCNA levels. A previous study has demonstrated that the expression of PCNA is about ten-fold higher in rats after ALPPS compared with the transection and left lateral lobe resection groups, and four-fold higher compared with the PVL group (24). Intriguingly, both Borger *et al.* and Otsuka *et al.* proposed that there may be other signaling pathways involved in the accelerated liver regeneration after ALPPS (25,26). Therefore, this current study performed bioinformatics analyses to screen the differentially expressed genes before and after ALPPS and PVL in rats. PCNA and MMP-centered gene clusters were identified. Consistently, MMP2 and MMP9 were found to be significantly downregulated in liver tissues of rats at postoperative day 4, and upregulated at day 10 by RT-qPCR in our study. Patients with nonalcoholic fatty liver, which may progress to cirrhosis, harboring high hepatic levels of MMP9 have been shown to be prone to disease progression (27).

Moreover, MMP2 and MMP9 are the most related MMPs that degrade normal liver matrix, thereby contributing to the pathogenesis of liver fibrosis, predominantly in response to liver injury (28). However, the relevance of MMP2 and MMP9 in ALPPS or cirrhosis remains largely unexplored.

In summary, this study suggested that ALPPS is more beneficial for rats with cirrhosis due to the rapid liver hypertrophy during days 1–4 post-surgery. PCNA and MMP2/9 may be responsible for liver regeneration after ALPPS in rats. The suggested mechanisms of rapid liver regeneration may contribute to understanding the multifactorial mechanisms underlying the ALPPS procedure. Nevertheless, these results should be verified using clinical data, and further basic research is warranted.

Acknowledgments

The authors would like to thank the Institute of Hepatobiliary Surgery, Faculty of Hepato-Pancreato-Biliary Surgery, Key Laboratory of Digital Hepatobiliary Surgery, Lab Tech, Pathology of Aerospace Center Hospital for their support and assistance in this study.
Funding: None.

Footnote

Reporting Checklist: The authors have completed the ARRIVE reporting checklist. Available at https://atm.amegroups.com/article/view/10.21037/atm-22-1312/rc

Data Sharing Statement: Available at https://atm.amegroups.com/article/view/10.21037/atm-22-1312/dss

Conflicts of Interest: All authors have completed the ICMJE uniform disclosure form (available at https://atm.amegroups.com/article/view/10.21037/atm-22-1312/coif). The authors have no conflicts of interest to declare.

Ethical Statement: The authors are accountable for all aspects of the work in ensuring that questions related to the accuracy or integrity of any part of the work are appropriately investigated and resolved. Animal experiments were performed under a project license (No. 20200511-JJJHZ-01) granted by the Medical Ethics Committee of Aerospace Center Hospital, in compliance with Chinese guidelines for the care and use of animals.

References

1. Byass P. The global burden of liver disease: a challenge for methods and for public health. BMC Med 2014;12:159.
2. Boudreault S, Chen J, Wu KY, et al. Self-management programmes for cirrhosis: A systematic review. J Clin Nurs 2020;29:3625-37.
3. Chan A, Kow A, Hibi T, et al. Liver resection in Cirrhotic liver: Are there any limits? Int J Surg 2020;82S:109-14.
4. Chan A, Zhang WY, Chok K, et al. ALPPS Versus Portal Vein Embolization for Hepatitis-related Hepatocellular Carcinoma: A Changing Paradigm in Modulation of Future Liver Remnant Before Major Hepatectomy. Ann Surg 2021;273:957-65.
5. Cavaness KM, Doyle MB, Lin Y, et al. Using ALPPS to induce rapid liver hypertrophy in a patient with hepatic fibrosis and portal vein thrombosis. J Gastrointest Surg 2013;17:207-12.
6. Schadde E, Ardiles V, Slankamenac K, et al. ALPPS offers a better chance of complete resection in patients with primarily unresectable liver tumors compared with conventional-staged hepatectomies: results of a multicenter analysis. World J Surg 2014;38:1510-9.
7. Alvarez FA, Ardiles V, Sanchez Claria R, et al. Associating liver partition and portal vein ligation for staged hepatectomy (ALPPS): tips and tricks. J Gastrointest Surg 2013;17:814-21.
8. García-Pérez R, Revilla-Nuin B, Martínez CM, et al. Associated Liver Partition and Portal Vein Ligation (ALPPS) vs Selective Portal Vein Ligation (PVL) for Staged Hepatectomy in a Rat Model. Similar Regenerative Response? PLoS One 2015;10:e0144096.
9. Li J, Girotti P, Königsrainer I, et al. ALPPS in right trisectionectomy: a safe procedure to avoid postoperative liver failure? J Gastrointest Surg 2013;17:956-61.
10. Moris D, Vernadakis S, Papalampros A, et al. Mechanistic insights of rapid liver regeneration after associating liver partition and portal vein ligation for stage hepatectomy. World J Gastroenterol 2016;22:7613-24.

11. Balci D, Sakamoto Y, Li J, et al. Associating liver partition and portal vein ligation for staged hepatectomy (ALPPS) procedure for cholangiocarcinoma. Int J Surg 2020;82S:97-102.
12. Schlegel A, Lesurtel M, Melloul E, et al. ALPPS: from human to mice highlighting accelerated and novel mechanisms of liver regeneration. Ann Surg 2014;260:839-46; discussion 846-7.
13. Schadde E, Hertl M, Breitenstein S, et al. Rat Model of the Associating Liver Partition and Portal Vein Ligation for Staged Hepatectomy (ALPPS) Procedure. J Vis Exp 2017;(126):55895.
14. Linecker M, Kambakamba P, Reiner CS, et al. How much liver needs to be transected in ALPPS? A translational study investigating the concept of less invasiveness. Surgery 2017;161:453-64.
15. Chan KS, Low JK, Shelat VG. Associated liver partition and portal vein ligation for staged hepatectomy: a review. Transl Gastroenterol Hepatol 2020;5:37.
16. D'Haese JG, Neumann J, Weniger M, et al. Should ALPPS be Used for Liver Resection in Intermediate-Stage HCC? Ann Surg Oncol 2016;23:1335-43.
17. Yang X, Yang C, Qiu Y, et al. A preliminary study of associating liver partition and portal vein ligation for staged hepatectomy in a rat model of liver cirrhosis. Exp Ther Med 2019;18:1203-11.
18. Madoff DC, Odisio BC, Schadde E, et al. Improving the Safety of Major Resection for Hepatobiliary Malignancy: Portal Vein Embolization and Recent Innovations in Liver Regeneration Strategies. Curr Oncol Rep 2020;22:59.
19. Daradics N, Olthof PB, Budai A, et al. The Role of Farnesoid X Receptor in Accelerated Liver Regeneration in Rats Subjected to ALPPS. Curr Oncol 2021;28:5240-54.
20. Zhang B, Meng F, Liu Y, et al. Inhibition of TGFbeta1 accelerates regeneration of fibrotic rat liver elicited by a novel two-staged hepatectomy. Theranostics 2021;11:4743-58.
21. Lopez-Lopez V, Robles-Campos R, Brusadin R, et al. ALPPS for hepatocarcinoma under cirrhosis: a feasible alternative to portal vein embolization. Ann Transl Med 2019;7:691.
22. Le Roy B, Dupré A, Gallon A, et al. Liver hypertrophy: Underlying mechanisms and promoting procedures before major hepatectomy. J Visc Surg 2018;155:393-401.
23. Taub R. Liver regeneration: from myth to mechanism. Nat Rev Mol Cell Biol 2004;5:836-47.
24. Shi H, Yang G, Zheng T, et al. A preliminary study of ALPPS procedure in a rat model. Sci Rep 2015;5:17567.
25. Borger P, Schneider M, Frick L, et al. Exploration of the Transcriptional Landscape of ALPPS Reveals the Pathways of Accelerated Liver Regeneration. Front Oncol 2019;9:1206.
26. Otsuka N, Yoshioka M, Abe Y, et al. Reg3α and Reg3β Expressions Followed by JAK2/STAT3 Activation Play a Pivotal Role in the Acceleration of Liver Hypertrophy in a Rat ALPPS Model. Int J Mol Sci 2020;21:4077.
27. Coilly A, Desterke C, Guettier C, et al. FABP4 and MMP9 levels identified as predictive factors for poor prognosis in patients with nonalcoholic fatty liver using data mining approaches and gene expression analysis. Sci Rep 2019;9:19785.
28. Arthur MJ. Fibrogenesis II. Metalloproteinases and their inhibitors in liver fibrosis. Am J Physiol Gastrointest Liver Physiol 2000;279:G245-9.

(English Language Editor: J. Teoh)

Cite this article as: Qin Y, Li C, Ge X, Zhang Q, Wei X, Liu R. MMP2/9 downregulation is responsible for hepatic function recovery in cirrhotic rats following associating liver partition and portal vein ligation for staged hepatectomy. Ann Transl Med 2022;10(8):468. doi: 10.21037/atm-22-1312

